KINETICS AND EQUILIBRIUM STUDIES OF THE DETOXIFICATION OF AQUEOUS SOLUTIONS OF PHENOLIC DERIVATIVES USING ACTIVATED CARBON

Abstract

In this study, activated carbon was prepared from coconut husk by chemical activation with potassium hydroxide. The activated carbon was used to detoxify aqueous solutions of p-nitrophenol and p-chlorophenol, by taking advantage of the physical adsorption of these phenolic derivatives on this adsorbent. Adsorption capacity of the adsorbent was dependent on the operating variables. The operating variables investigated were adsorbent dose, initial concentration of adsorbate, contact time and temperature. Optimal adsorption was observed at adsorbent dose of 0.2 g and contact time of approximately 2 hours for both adsorbates. The highest uptake capacity of 125 ppm and 71.43 ppm were observed for p-nitrophenol and p-chlorophenol respectively on the adsorbent. In both cases, adsorption capacity decreases with increase in temperature. Kinetic measurements showed that the process was uniform and rapid. Kinetic data were modelled using the pseudo-first-order and pseudo-second-order kinetic equations. The pseudo-second-order equation was the best applicable model to describe the adsorption process of 4-chlorophenol and 4-nitrophenol on the adsorbents. Equilibrium isotherm data were analyzed using the Langmuir isotherm. Results of equilibrium analysis suggest that the adsorption process is consistent with the Langmuir isotherm model, which is indicative of a monolayer adsorption of each of the adsorbate on the adsorbent.

Keywords: *Activated Carbon, p-nitrophenol, p-chlorophenol, Kinetic Measurements, Chemical Activation*

1.0 INTRODUCTION

1.1 Phenolic derivatives

Phenol is widely used for the commercial production of various resins (Joseph et al., 2024), including phenolic resins which are used as construction materials for automobiles and appliances, epoxy resins and adhesives, and polyamide for various applications (Anwar & Li, 2024; Pizzi & Ibeh, 2022). Phenolic compounds may be present in our environments, plant seeds like Almonds (Moreno *et al*.,2001; Patrick *et al*., 2024). Phenolic pollutants occur in wastewater from several industries, such as high-temperature coal conversion, petroleum refining, resin, and plastics (Zhu et al., 2024). At certain concentrations, aromatic hydroxyl compounds are considered priority pollutants since they harm organisms, especially humans and aquatic life (Panigrahy et al., 2022). Phenolic compounds are classified as highly toxic to humans and aquatic life (Ramos et al., 2021). Para-Nitro phenol (P-Nitro phenol) is one of the many phenol derivatives known to be persistent, bioaccumulative, and highly toxic (Anjum et al., 2022). It can enter the human body through all routes, and its toxic action is similar to aniline (Mir et al., 2023).

P- nitro phenol aids the conversion of hemoglobin to methemoglobin (Yadav & Maurya, 2022); it causes the oxidation of iron (II) to iron (III), which makes hemoglobin unable to transport oxygen in the body (Szafran et al., 2023). Therefore, the complete removal of p-Nitro phenol and other derivatives or, in some cases, the reduction of its concentration in wastewater to an acceptable level has become a significant challenge(Sivaraman et al., 2022). In the following sections, I will briefly describe the phenolic derivatives studied in this work.

1.1.1 Nitrophenols

Para-nitrophenol (PNP) irritates the eyes, skin, and respiratory tract. It has a delayed interaction with blood and forms methemoglobin, which is responsible for methemoglobinemia. This can potentially cause cyanosis, confusion, and unconsciousness(Vallant, D, 2016). When ingested, it causes abdominal pain and vomiting. Prolonged contact with the skin may cause an allergic response(Msagati, 2017). Nitrophenols, particularly 2-nitrophenol and 4-nitrophenol, are formed when

phenol reacts with nitrite ions in water (Marussi & Vione, 2021). The reactions proceed under the influence of UV irradiation (sunlight) and in a wide range of pH values(Lojo-López et al., 2021; Brillas, 2020). Nitrophenols in the atmosphere are usually determined in low concentrations of some ng /dm^3; however, intense pollution of air due to industrial emissions leads to an increase of Nitrophenols concentrations up to 320 ng/dm^3 (Adeniji et al., 2021).

Nitrated phenols are used in dyes, solvents, plastics, and explosives production (Gijjapu & Nazal, 2023) and are formed due to electric, electronic, and metallurgic industrial activities (Husieva, 2021).

MonoNitrophenols, 3-methyl-4-nitrophenol, and 4-nitro-3-phenylphenol reach the environment through vehicular emissions (Zaki et al., 2015). The kinetic study of how these substances are absorbed gives us a better understanding of how to reduce or even eliminate the amount of PNP people consume using cheap absorbents available in the environment (Fernández et al., 2020).

1.1.2 *Chlorophenols*

Chlorophenols (CPs) are harmful toxic substances because they easily penetrate the skin and epithelium, leading to damage and necrosis (Al-Ahmadi, 2022). Chlorophenols are found in the environment from a variety of sources such as industrial waste, pesticides, and insecticides, or by degradation of complex chlorinated hydrocarbons (Adetunji et al., 2021).

Chlorophenols are the most widespread and significant phenols group (Garba et al.,2019). They are formed in the environment by chlorinating mono- and poly-aromatic compounds present in soil and water. Exposure to chlorophenols may occur *via* ingestion, inhalation, or dermal absorption(Adeola, A, 2018). The general population is thought to be exposed mainly through the ingestion of food and drinking water. However, non-occupational exposure by inhalation may be significant if chlorophenols are used for extensive treatment of the interior of houses (Skowroń, J, 2020).

Para-chlorophenol (PCP) is a white crystal with a strong phenol odor, slightly soluble to soluble in water, it is non-combustible. It is used as an intermediate in the organic synthesis of dyes and drugs. Inhalation causes headache, dizziness, and weak pulse.

Ingestion causes irritation of mouth and stomach; headache, dizziness, weak pulse. Contact with eyes causes severe irritation and burning; if absorbed, causes same symptoms as inhalation (Underwood, 2018). Due to the hazardous nature of 4-Chlorophenol and its ease of diffusion into the skin, it has become imperative that a faster and efficient method of detoxification is identified (Irshad et al., 2023).

Table 1 below illustrates the structure and chemical formula of the compounds under investigation which are derivatives of the first structure i.e. phenol

Table .1 Phenol and its derivatives studied in this work

Phenolic derivatives	Structure	Chemical formula
Phenol	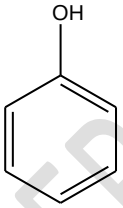	C_6H_6O
4-chlorophenol	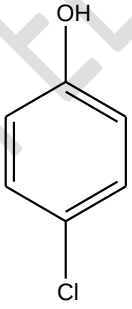	C_6H_5OCl
4-Nitrophenol	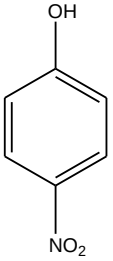	$C_6H_5NO_3$

In removing these phenolic derivatives from aqueous solutions, it is necessary that a good adsorbent of these compounds is employed. Activated carbon materials are effective in removing

pollutants (both gaseous and liquid). The advantage of activated carbon materials as adsorbents is that the treated effluent is of high quality, the design of the process is simple, and the operation of the process developed or adopted is easy (Azari et al., 2022). A coconut shell based activated carbon will have a predominance of pores in the micropore range and this account for 95% of the available internal surface area (Trisunaryanti et al., 2022). Such a structure has been found ideal for the adsorption of small molecular weight species and applications involving low contaminant concentrations.

In this research, the choice of coconut shell is due to its internal surface area which is between micropore and mesopore and is found to be ideal for the adsorption of small molecular weight species such as p-chlorophenol (Molecular weight. 128.5 g/mol) and p-Nitrophenol (Molecular weight. 139g/mol) in contrast to that of wood.

2.0 MATERIALS AND METHODS

2.1 Materials

Sodium Hydroxide, Potassium Hydroxide, Hydrochloric acid were obtained from Merck. P-Nitrophenol 99.9% was obtained from BDH England. The chlorophenol was obtained from Merck.All the reagents were of analytical grade and were used as received from the suppliers without further purification.

Coconut husk used was obtained locally.

2.2 Equipment

Boss Multi-purpose Pulveriser, analytical balance, electric stirrer, electric oven, electric furnace, thermostat water bath, UV-visible spectrometer Genesis10-S model, volumetric flasks, glass rod, 2 ml micro pipette and measuring cylinders.

2.3 Preparation and activation of activated carbon from coconut husk

The chemical activation of coconut husk was done following the method already reported by Sujiono et al., 2022. The coconut husk was cut into small sizes and dried in an oven overnight at 100 ^{0}C. It was then pulverized into tiny particles and sieved. Washing was done with dilute hydrochloric acid and distilled water to remove materials adhering to these particles and oven-dried for six hours. These materials were impregnated with KOH solution (1.5 M) with an impregnating ratio (w/w) of 4:1(KOH: char) after soaking for about 4 hours. It was dried before carbonization, and activation was carried out simultaneously at 550 ^{0}C for about 1 hour. The resulting material was allowed to cool after about 12 hours, washed with 0.05 M dilute HCl, followed by distilled water, and dried for about 6 hours. The sample was stored in an airtight container for further use.

2.4 Preparation of solutions

The methods used in preparing the solutions used in this research work are reported below. 0.1 M HCl was prepared by diluting 9.0 ml of concentrated Hydrochloric acid (S.G 1.18, 36%) in 200 ml of distilled water and made up to 1000 ml in a 1 L volumetric flask. 1.5M solution of Potassium Hydroxide was prepared by dissolving 79.5g of KOH pellets in 200 ml of distilled water and made up to 1000 ml in a 1 L volumetric flask**.** 0.05 M solution of Sodium Hydroxide was prepared by dissolving 0.2 g of NaOH pellet in 100 ml of distilled water.

2.4.1 ***Preparation of test solution of 4-Nitrophenol***

The test solutions were prepared by diluting a stock solution of 4-Nitrophenol to the desired concentrations. A stock solution of 4-Nitrophenol was obtained by dissolving 1.0 g of 4-Nitrophenol (obtained from BDH, England), in distilled water and diluted to 1000 ml. Several dilutions of stock solution were made to obtain specific concentrations required for the adsorption study.

2.4.2 ***Preparation of test solution of 4-Chlorophenol***

The test solutions were prepared by diluting a stock solution of chlorophenol to the desired concentrations. A stock solution of chlorophenol was obtained by dissolving 1.0 g of 4-

chlorophenol (obtained from Merck, India), in distilled water and diluted to 1000 ml. Serial dilutions of stock solution were made to obtain specific concentrations required for the adsorption study.

2.3 Analytical measurement of the phenolic derivatives

The standard calibration curve of known concentrations of 4-Nitrophenol and 4-chlorophenol was plotted by finding out the absorbance at the characteristic wavelength of λ_{max} =226 nm for 4-chlorophenol and λ_{max} = 361 nm for P-Nitrophenol. A spectrophotometer (Genesis10-s UV/Vis) was used for the calibration plot, which showed a linear variation of absorbance up to 20 mg/l concentration. Therefore, the samples with higher concentration of phenol were diluted with distilled water.

2.3 Batch adsorption procedure

All the batch adsorption experiments were performed in a electrical stirrer and a thermostat water bath 250 ml conical flasks containing 50 ml each of the test solutions whose concentrations are dependent on the parameter under investigation. Experiments were performed at room temperature (30 ^{0}C). The pH of the solution was maintained natural for all the parameters investigated, i.e. adsorbent doses, temperature, contact time and concentration. All solution samples post adsorption was filtered through Whatman No 1 (with diameter 110 mm X 125 mm) filter paper and centrifuged for five (5) minutes. The concentrations of 4-Nitrophenol and 4-Chlorophenol in the treated samples were determined by UV spectrophotometer.

The amount of the phenolic derivative adsorbed per unit mass of the adsorbent was evaluated by using the following equation,

$q_e = C_o - C_e$ Scheme 1

Where

q_e = amount of phenol adsorbed at equilibrium

C_o = initial concentration of the phenolic derivative

C_e = equilibrium concentration of the phenolic derivative

The percentage removal of phenolic derivative was calculated by the following equation.

$$\%R = [\frac{Co-Ct}{Co}] \times 100 \qquad \text{Scheme 2}$$

2.4 Kinetics models

Kinetics models are used to examine the rate of the adsorption process and potential rate controlling step. In the present work, the kinetic data obtained from batch studies have been analyzed by using pseudo-first-order and pseudo-second-order models. The first order equation of Lagergren is generally expressed as follows,

$$\frac{dq}{dt} = k_1 (q_e - q_t) \qquad \text{Scheme 3}$$

Where q_e and q_t are the amounts of phenolic derivative adsorbed at equilibrium and at time t (min), respectively, and k_1 is the rate constant of pseudo-first-order sorption (min^{-1}). The linearized form of above equation is given as,

$$\text{In } (q_e - qt) = \text{In}q_{ce} - k_1 t \qquad \text{Scheme 4}$$

q_{ce} is the calculated equilibrium adsorption capacity

A plot of ln ($q_e - q_t$) against t should give a linear relationship with the slop k_1 and intercept of $\ln q_{ce}$.

The pseudo-second-order kinetic rate equation is expressed as follows,

$$\frac{dq}{dt} = k_2 (q_e - q_t)^2 \qquad \text{Scheme 5}$$

Where k_2 is the rate constant of pseudo-second-order sorption (g mg^{-1} min^{-1}). The linearized form of above equation becomes,

$$\frac{t}{q_t} = \frac{1}{k_2 \, q_e^2} + \frac{1}{q_{ce}} t \qquad \text{Scheme 6}$$

If the second order kinetic equation is applicable, the plot of t/q_t against t should give a linear relationship. The q_{ce} and k_2 can be determined from the slope and intercept of the plot.

RESULTS AND DISCUSSION

3.1 Adsorbent (CHAC) preparation

The desired adsorbent i.e. CHAC was prepared by following standard methodologies reported in the previous chapter. The percentage yield was calculated using eq.3.1below;

Percentage yield (%R) = $\frac{Wchar}{Wraw}$ x 100 Scheme 6

Where,

W_{CHAR} Weight of char produced after carbonization and

W_{RAW} Weight of raw material before carbonization

Percentage yield (%R) = $\left(\frac{17.447}{31.753}\right)$ x 100 = 54.95%

Therefore the yield of **CHAC** obtained was 54.95%.

3.2 Study of the effects of various parameters on adsorption of 4-Nitrophenol onto CHAC

Adsorption in liquid phase is affected by various chemical and physical parameters such as concentration, type of specie being adsorbed, adsorbent dose, pH, contact time and temperature. This work investigates the effect of adsorbent dose, concentration, contact time and temperature on the adsorption of phenolic derivatives onto CHAC.

3.2.1 *Effect of adsorbent (CHAC) dose on adsorption*

This study was done in order to find out the optimal adsorbent dose of CHAC. The effect of CHAC on the amount of 4-Nitrophenol solution removed was investigated by contacting 20 ml of 4-Nitrophenol solution, of initial concentration of 100 ppm with different weighed amounts (0.02 g, 0.05 g, 0.1 g, 0.12 g, and 0.2 g) of CHAC in stoppered conical flasks. Each sample was then agitated for 1h at the natural pH of solution. The supernatants were then filtered using Whatman filter paper 1 grade and subsequently centrifuged for 5mins and analyzed.

The result obtained are shown in table 2

Table 2 Effect of adsorbent dose on adsorption PNP

Mass of CHAC, g	Initial conc. Ppm	absorbance	Final conc. q_e (ppm)	Amount adsorbed (ppm)
0.02	100	1.343	55.95	44.05
0.05	100	1.321	55.00	45.00
0.10	100	1.357	56.36	43.64
0.12	100	1.309	47.85	52.15
0.20	100	1.237	44.96	55.04

The result from the above table shows increase in the amount adsorbed as the amount of adsorbent increases.

A plot of q_e and % of adsorbent removed was plotted on same axis against adsorbent dose. The plot is shown in fig. .1

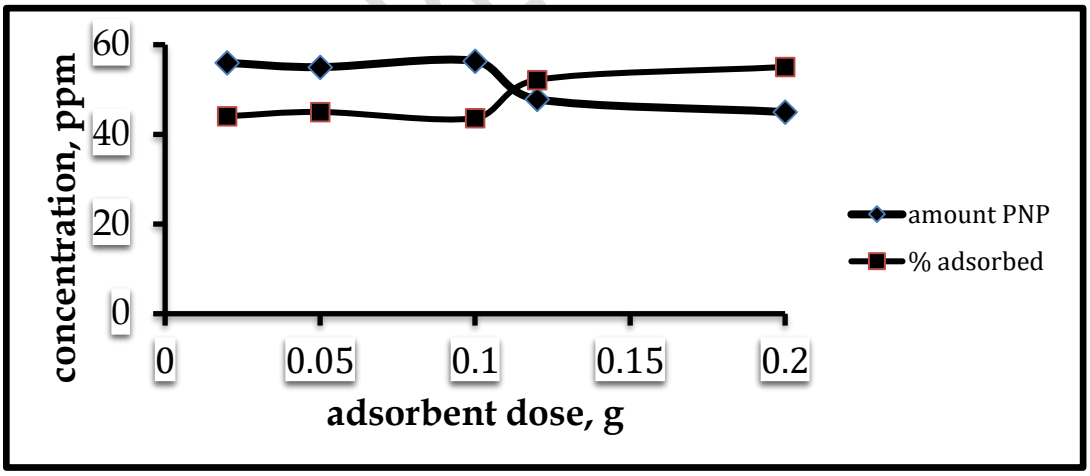

Fig *.1 Effect of adsorbent (CHAC) dose on adsorption*

In the graph above, the percentage removal of phenol increased with the increase in adsorbent dosage. This can be attributed to increased adsorbent surface area and availability of more adsorption sites resulting from the increase adsorbent dosage. But the amount of 4-Nitrophenol

adsorbed per unit mass of CHAC decreased with increase in adsorbent dosage, because for the same 4-Nitrophenol concentration, a large number of adsorption sites with the increment of CHAC dose.

3.3.2 *Effect of Contact time for adsorption of P-Nitrophenol (PNP) onto CHAC*

To investigate the effect of contact time on adsorption of 4-Nitrophenol (C_o =100 ppm), the batch experiments were carried out in a series of conical flasks with a constant CHAC dose of 0.2 g in 50 ml of 100 ppm. These flasks were agitated in electric stirrer for 20, 40, 60, 80, 100 and 120 minutes at the natural pH in all the samples. The supernatants were then filtered using Whatman filter paper No 1 grade and centrifuged for 5 minutes. The concentration of 4-Nitro-phenol in supernatant was measured for all the samples. The results obtained are shown in table 3.

Table 3. Table Effect of contact time on adsorption of PNP

Time, mins	**Initial conc. ppm**	**absorbance**	**Final conc. C_e (ppm)**	**Amount adsorbed q_e (ppm)**
20	100	1.371	55.05	44.95
40	100	1.349	51.89	48.11
60	100	1.246	49.92	50.08
80	100	1.217	41.80	58.2
100	100	1.155	36.16	63.84
120	100	1.129	35.35	64.65

The q_e was evaluated for all the samples and the graph of q_e versus time is shown in Fig. .2

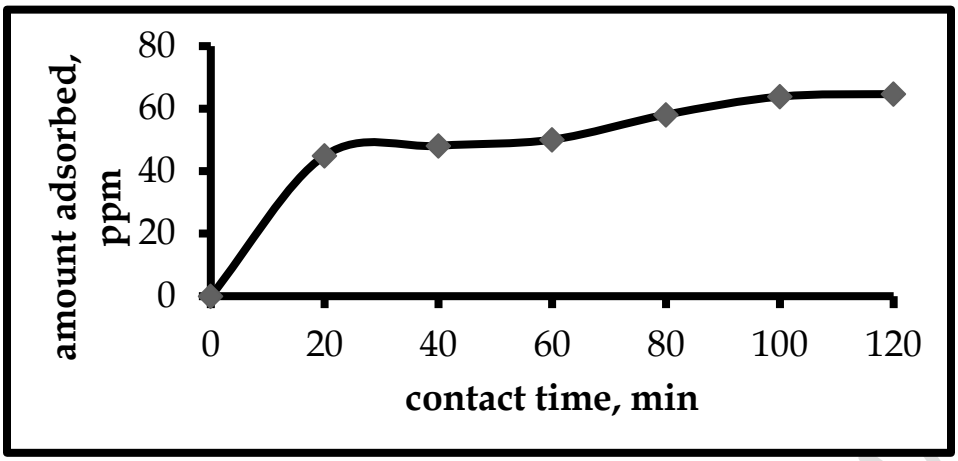

Fig. 2 Effect of Contact time for adsorption of 4-Nitrophenol onto CHAC

From the above graph, it was found that at the initial stage, the rate of adsorption of p-Nitrophenol (PNP) rises sharply, indicating that there are plenty of readily accessible sites. Thereafter, amount of adsorption reduces gradually. As time proceeds this percentage gradient is reduced due to the accumulation of PNP particles in the vacant sites, leading to a decrease in the sorption rate at the later stages. Equilibrium was observed after 120 minutes as the amount of PNP adsorbed was approximately the same after 100 minutes.

3.2.3 Effect of concentration on adsorption of PNP

To study the effect of initial PNP concentration, experiments were carried out in different conical flasks with a fixed adsorbent dose of 0.2 g at varying PNP concentrations of 50 ppm, 100 ppm, 150 ppm, and 200 ppm taking 50 ml of each solution at room temperature. The conical flask was agitated for 2 hour. Post adsorption, the supernatant was collected and filtered using Whatman filter paper No 1 grade and then centrifuged for 5 minutes. Filtered supernatant was analyzed using spectrophotometer and a graph was plotted with q_e versus time. The adsorption data for the uptake of PNP versus initial concentrations is represented in table 4

Table 4 Effect of concentration on adsorption of PNP

Initial conc. ppm	absorbance	Final conc. ppm	Amount adsorbed, ppm	Percentage adsorbed %
50	0.555	24.89	25.11	50.22
100	1.129	35.35	64.65	64.65
150	1.423	61.35	88.65	59.10
200	1.778	76.55	123.45	61.72
250	1.972	89.45	160.55	64.22

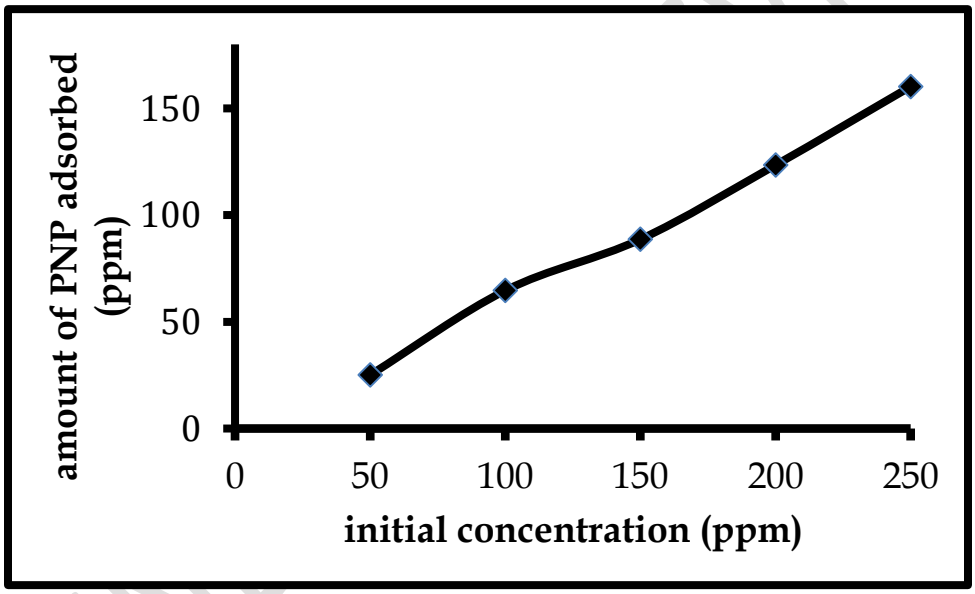

Fig .3 effect of initial concentration on adsorption

From the above graph, increase in adsorbate concentration result in an increase in adsorption process. This trend could also suggests that increase in adsorbate concentration results in increase in number of available molecules per binding site of the adsorbent thus bringing about a higher probability of binding of molecules to the adsorbent (i.e. the probability of chemical interaction between the adsorbent and the adsorbate is enhanced by reason of the high availability of molecules of adsorbate).

3.2.*4 Effect of temperature on adsorption of PNP*

To elucidate the effect of temperature on adsorption, 50 ml each of 100 ppm solution was transferred into various 250 cm^3 flask containing 0.2 g each of the adsorbent, corked and labeled for different temperatures 30 ^oC, 40 ^oC, 50 ^oC, and 60 ^oC respectively. The mixture was stirred for 1 hour and heated in a thermostat water bath to the appropriate temperature in a water bath. At the right temperature, the content of the each of the flask was removed, filtered using Whatman filter paper No 1 grade and then centrifuged for 5 minutes and the concentration of the PNP was determined using UV-VIS spectrometer. The results obtained are shown in table 5

Table 5 Effect of temperature on adsorption of PNP

Temperature , K	**Initial conc. ppm**	**absorbance**	**Final conc. ppm**	**Amount adsorbed ppm**
303	100	1.100	49.36	50.64
313	100	1.191	49.77	50.23
323	100	1.411	63.05	36.95
333	100	1.722	70.65	29.35

The graph below shows the relationship between temperature in Kelvin and amount adsorbed.

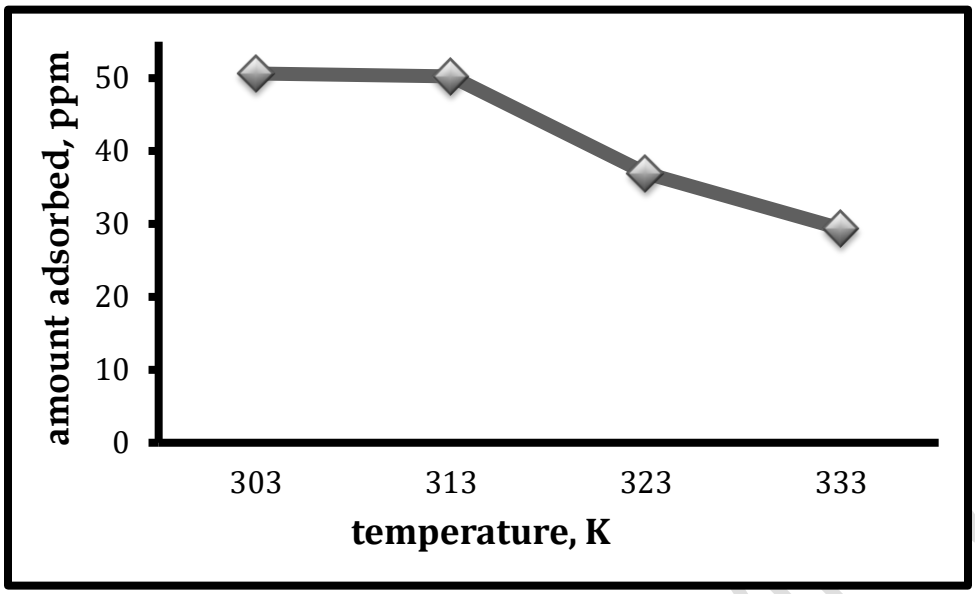

Fig 4 Effect of temperature on adsorption of PNP

It is evident from Fig. 4 that the amount of PNP adsorbed decreases with temperature thus suggesting that adsorption is favored at lower temperatures. At high temperature kinetic energy of adsorbate (PNP) is so high that they do not bind with the active sites available on the CHAC surface. This suggests that the process of adsorption is exothermic.

3.3 Study of the effects of various parameters on adsorption of 4-chlorophenol onto CHAC

3.3.1 *Effect of concentration on adsorption of P-chlorophenol (PCP)*

To study the effect of initial PCP concentration, experiments were carried out in different conical flasks with a fixed adsorbent dose of 0.2 g at varying PCP concentrations of 50 ppm, 100 ppm, 150 ppm, and 200 ppm taking 50 ml of each concentration at room temperature. The conical flask was agitated for 2 hours. Post adsorption, the supernatant was collected and filtered using Whatman filter paper No 1 grade and then centrifuged for 5 minutes. Filtered supernatant was analyzed using spectrophotometer. The results obtained are shown in table 6.

Table 6 Effect of concentration on adsorption of PCP

Initial conc. (ppm)	absorbance	Final conc. (ppm)	Amount adsorbed (ppm)	Percentage adsorbed %
50	1.164	21.59	28.41	56.82
100	1.763	32.69	67.31	67.31
150	2.363	48.27	101.73	67.82
200	2.664	49.40	150.06	75.03
250	2.781	51.61	198.39	79.36

The graphical illustration of the uptake of PCP versus initial concentrations is represented in fig. .5

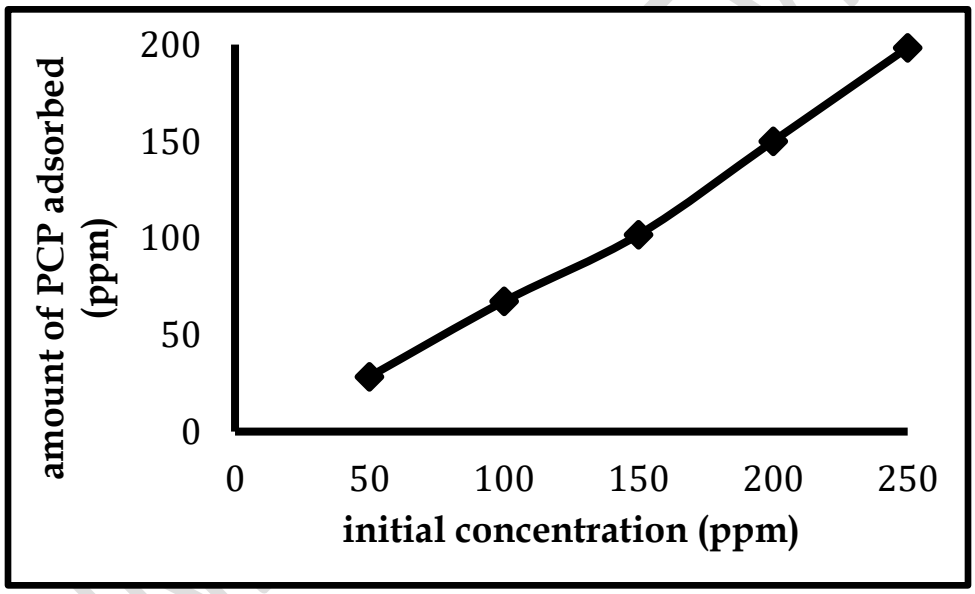

Fig 5 Effect of initial concentration on adsorption of PCP

It is evident from the above graph that, increase in adsorbate concentration result in an increase in adsorption process. This trend could also suggests that increase in adsorbate concentration results in increase in number of available molecules per binding site of the adsorbent thus bringing about a higher probability of binding of molecules to the adsorbent (i.e. the probability

of chemical interaction between the adsorbent and the adsorbate is enhanced by reason of the high availability of molecules of adsorbate in solution).

3.3.2 Effect of contact time on adsorption of PCP

To investigate the effect of contact time on adsorption of PCP (C_o =100 ppm), the batch experiments were carried out in a series of conical flasks using 50 ml of the above concentration with a constant CHAC dose of 0.2 g in all the samples. These flasks were agitated in electric stirrer for 20, 40, 80, 100 and 120 minutes at the natural pH in all the samples. The supernatants were then filtered using Whatman filter paper No 1 grade and centrifuged for 5 minutes. The concentration of PCP in supernatant was measured for all the samples. The table of result is shown in table 7

Table 7 Effect of contact time on adsorption of PCP

Time, mins	**Initial conc**	**absorbance**	**Final conc. ppm**	**Amount adsorbed , ppm**	**Percentage adsorbed %**
20	100	2.832	52.35	47.65	47.65
40	100	2.361	48.67	51.33	51.33
60	100	2.282	45.26	54.74	54.74
80	100	2.188	40.58	59.42	59.42
100	100	1.887	33.85	66.15	66.15
120	100	1.763	32.69	67.31	67.31

The graphical representation of the above result is shown in fig 6 below.

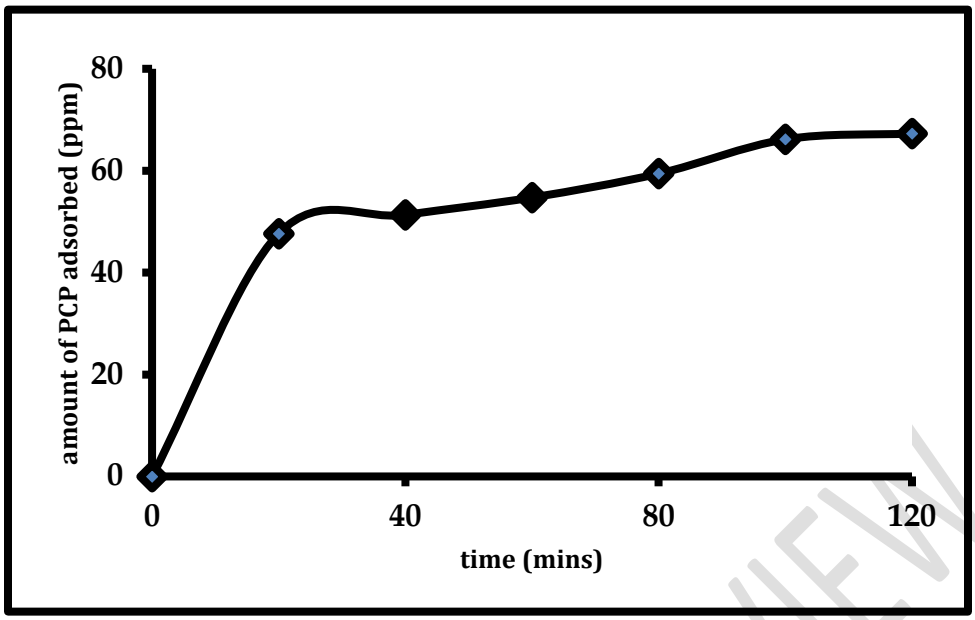

Fig 6 effect of contact time on adsorption of PCP

Based on the above graph, it was found that at the initial stage, the rate of adsorption of PCP rises sharply; indicating that there are plenty of readily accessible sites and gradually reduces as the adsorption capacity. As time proceeds the percentage gradient is reduced due to the accumulation of PCP particles in the vacant sites leading to a decrease in the sorption rate at the later stages. Equilibrium was observed after 120 minutes as the amount of PCP adsorbed was approximately the same after 100 minutes.

3.3.3 Effect of temperature on adsorption of PCP onto CHAC

To elucidate the effect of temperature on adsorption, 50 ml of 100 ppm solution was transferred into various 250 cm^3 flask containing 0.2 g each of the adsorbent, corked and labeled for different temperatures 30 ^{0}C, 40 ^{0}C, 50 ^{0}C, and 60^{0}C respectively. The mixture was stirred for 1 hour and heated in a thermostat water bath to the appropriate temperature in a water bath. At the right temperature, the content of the each of the flask was removed, filtered using Whatman filter paper No 1 grade and then centrifuged for 5 minutes and the concentration of the PCP was determined using UV-VIS spectrometer. The results obtained are shown in table 8

Table 8 Effect of temperature on adsorption of PCP

Temperature , K	Initial conc. (ppm)	absorbance	Final Conc. (ppm)	Amount adsorbed , ppm
303	100	1.482	27.48	72.52
313	100	1.582	29.35	70.65
323	100	1.796	33.35	66.65
333	100	1.983	36.77	63.23

The graph below shows the relationship between temperature in Kelvin and amount adsorbed

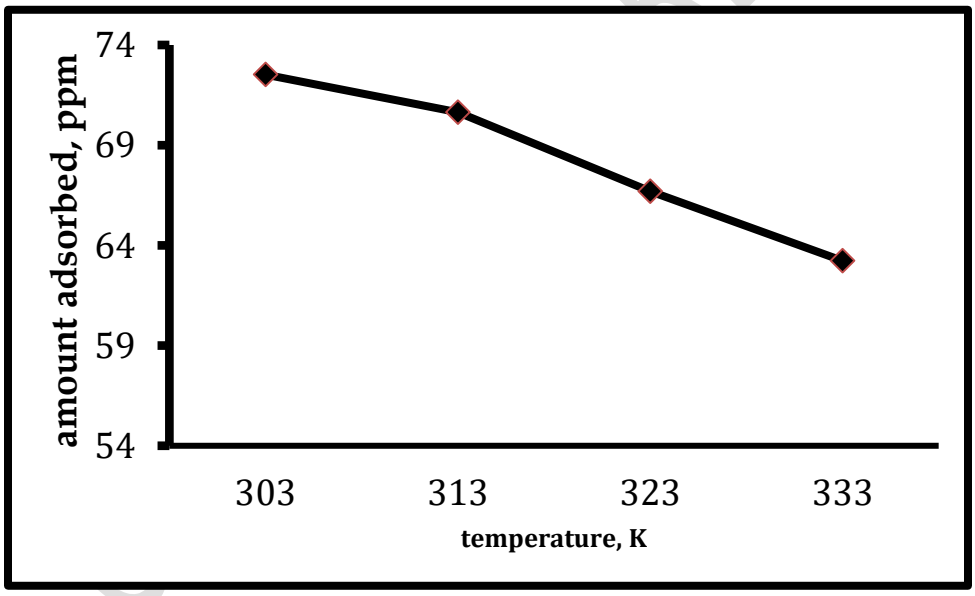

Fig 7 effect of temperature on adsorption of PCP onto CHAC

It is evident from Fig. 7 that the value of maximum adsorption capacity q_e decreases with increase in temperature thus suggesting that adsorption is favored at lower temperatures. At high temperature kinetic energy of adsorbate PCP is so high that they do not bind with the active sites available on the CHAC surface. This is similar to the result obtained for PNP.

3.4 Adsorption equilibrium study

Equilibrium study on adsorption provides information on the capacity of the adsorbent. An adsorption isotherm is characterized by certain constant values, which express the surface properties and affinity of the adsorbent and can also be used to compare the adsorptive capacities of the adsorbent for different pollutants.

Equilibrium study was investigated using Langmuir adsorption model.

3.4.1 Langmuir isotherm

The most widely used isotherm equation for modelling of the adsorption data is the Langmuir equation, which is valid for monolayer sorption onto a surface with a finite number identical site and is given by following equation,

$$\mathbf{q_e} = \frac{q_o K_l\, Ce}{1+K_l\, Ce} \qquad \text{Scheme 7}$$

Where q_o and K_l are Langmuir parameters related to maximum adsorption capacity and equilibrium constant of adsorption, respectively. C_e is the equilibrium concentration in the aqueous solution and q_e is the equilibrium adsorption capacity of adsorbent. The linearized form of Langmuir equation can be written as,

$$\frac{1}{q_e} = \frac{1}{q_o} + \frac{1}{k_1\, q_0} \mathbf{x} \frac{1}{C_e} \qquad \text{Scheme 8}$$

The Langmuir constant q_0 and K_l can be calculated by plotting $1/q_e$ versus $1/C_e$.

3.4.2 Adsorption equilibrium study for PCP-CHAC system

The data obtained for the adsorption study of 4-chlorophenol is shown in the table 9

Table 9 Langmuir adsorption study of 4-chlorophenol on CHAC

Initial conc. ppm	Final conc. C_e, ppm	Amount adsorbed, q_e, ppm	1 / C_e	1 / q_e
50	21.59	28.41	0.0463	0.0352
100	32.69	67.31	0.0306	0.0149
150	48.27	101.73	0.0207	0.0098
200	49.40	150.06	0.0202	0.0067
250	51.61	198.39	0.0194	0.0050

The graphical illustration of the above result is presented in fig. 8

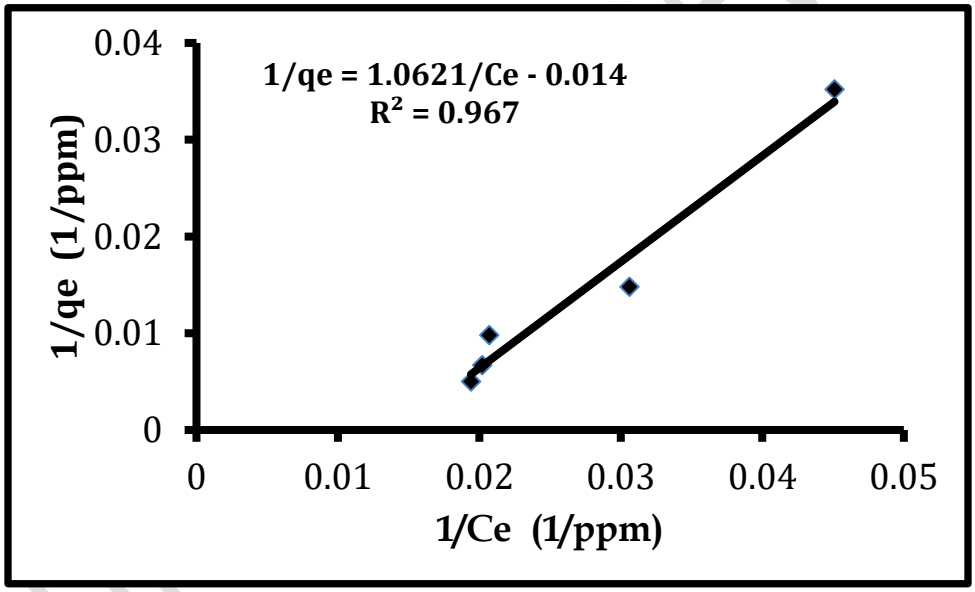

Fig. .8 Langmuir isotherm plot of PCP-CHAC adsorption system at 298K

From above plot,

$\frac{1}{q_e} = \frac{1}{q_o} + \frac{1}{k_1\ q_0} \mathbf{x} \frac{1}{C_e}$ Scheme 9

$1/q_o$ = -0.014 = intercept

$|qo|$ = 71.43 ppm

The above result represents the magnitude of the maximum Langmuir adsorption capacity of the adsorbent.

Also, $1/(q_o k_l)$ = 1.062 = slope

$k_l = \frac{1}{q_o} \text{x} \frac{1}{1.062}$

k_l = 0.014 x 0.942 hence, k_l = 0.013 ppm^{-1}

The above result shows that Langmuir constant of adsorption k_l is 0.013 ppm^{-1}

3.4.3 Adsorption equilibrium study for PNP-CHAC system

The Langmuir adsorption data of 4-Nitrophenol on CHAC is represented in the table 10

Table 10 Langmuir adsorption study of 4-Nitrophenol on CHAC

Initial conc. Ppm	**Final conc., C_e, ppm**	**Amount Adsorbed. q_e, ppm**	**1/qe**	**1/ C_e**
50	24.89	25.11	0.0398	0.0402
100	35.35	64.65	0.0155	0.0283
150	61.35	88.65	0.0113	0.0163
200	76.55	123.45	0.0081	0.0131
250	89.45	160.55	0.0062	0.0112

Graphically, the result is highlighted below (fig. 9), the plot of $1/q_e$ against $1/C_e$ gave a straight line graph whose slope and intercept can be used to evaluate q_o, the maximum adsorption capacity and k_l, Langmuir constant of adsorption.

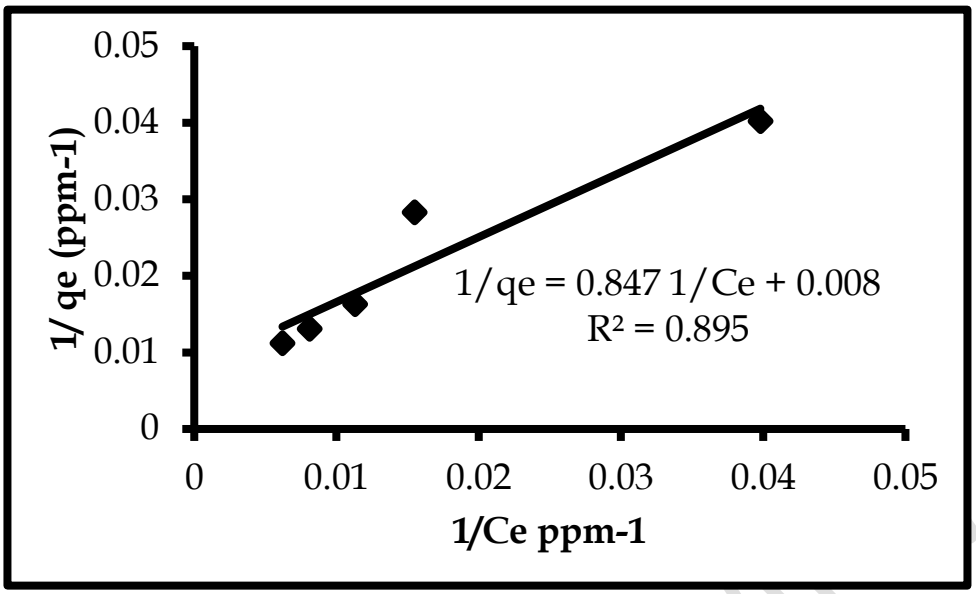

Fig 9 ***Langmuir isotherm plot of PNP-CHAC adsorption system at 298K***

From the above graph,

$\frac{1}{q_e} = \frac{1}{q_o} + \frac{1}{k_1\ q_0} \mathbf{x} \frac{1}{C_e}$

$1/q_o = 0.008$ = intercept

$q_o = 125$ ppm

The above result represents the maximum Langmuir adsorption capacity of the adsorbent.

Also,

$1 / (q_o k_l) = 0.847$ = slope

$k_l = \frac{1}{q_o} x \frac{1}{0.847}$

$k_l = 0.008 \times 1.1806$

$k_l = 000944\ ppm^{-1} = 9.44x10^{-3}\ ppm^{-1}$

The above result shows that Langmuir constant of adsorption k_l is $9.44x10^{-3}\ ppm^{-1}$

The Summary of Langmuir isotherm parameters for sorption of PNP and PCP onto CHAC are shown in table 11 below

Table 11 summary of Langmuir adsorption study

Adsorbate system	Max. adsorption capacity, q_o (ppm)	Adsorption energy , K_L, ppm^{-1}	Regression coefficient R^2
PNP-CHAC	125	000944	0.895
PCP-CHAC	71.43	0.013	0.968

From the above tables it is clear that the equilibrium data for 4-chlorophenol were very well fitted to Langmuir isotherm as reported by Ekpete et al., 2011 and Gbatbandhe *et al.,* 2009. 4-Nitrophenol also fitted well in the Langmuir isotherm. The correlation coefficient values for Langmuir isotherms are also high. The best fit of equilibrium data observed in the Langmuir isotherm expression predicts a monolayer coverage of 4-chlorophenol and 4-nitrophenol onto CHAC, with the maximum sorption capacity of 71.43 ppm and 125 ppm for 4-nitrophenol respectively.

3.5 Adsorption kinetics study

For the kinetics study, pseudo-first-order and pseudo-second-order models were considered. The various results obtained from this study are represented below.

3.5.1 ***Pseudo-first-order kinetics of PNP-CHAC system***

The linearized form of the pseudo-first-order kinetics equation is reported in 2.4 From that equation it is clear that, a plot of ln (q_e -q_t) against t (mins) should give a linear relationship with the slope k_1 and intercept of lnq_e. The q_e value for PNP was taken as 64.65 ppm, the amount of PNP adsorbed at equilibrium as previously reported. The Pseudo-first-order kinetics of PNP-CHAC system is given below,

Table 12 pseudo first order kinetics of PNP-CHAC system

q_e = 64.65 constant for all the data: the amount of PNP adsorbed at equilibrium

t(mins)	Adsorption capacity of PN t, q_t, ppm	q_e-q_t	ln (q_e-q_t)

20	44.950	19.70	2.980
40	48.112	16.54	2.805
60	50.080	14.45	2.671
80	58.200	6.45	1.864
100	63.160	0.81	-0.210

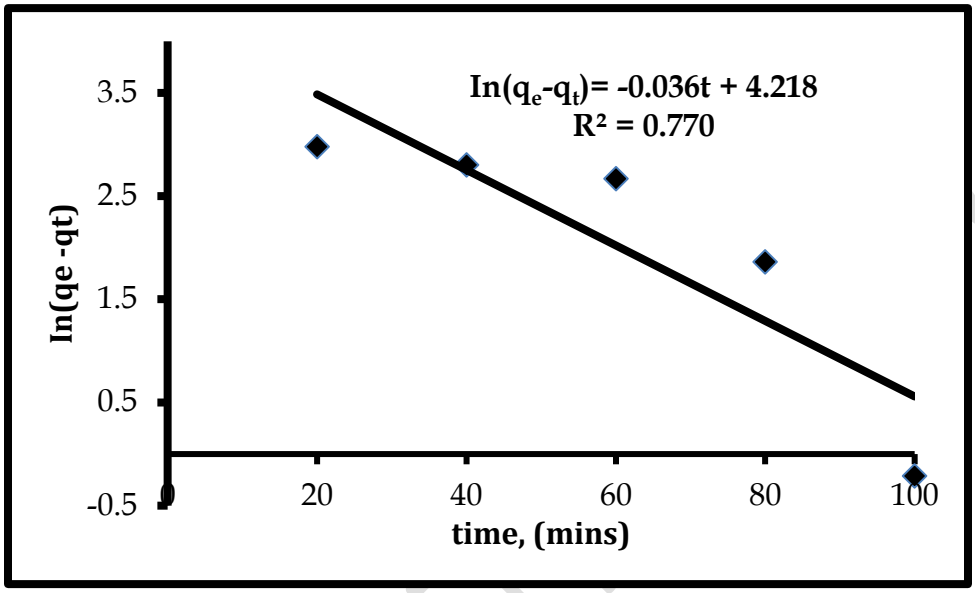

Fig 10 pseudo first order kinetics of PNP on CHAC

From the above graph, comparing the two linear equations,

In $(q_e - qt) = Inq_{ce} - k_1 t$

In $(q_e - q_t) = -0.036t + 4.218$

$-k_1 = -0.036$

$k_1 = 0.036$ ppm/min

Also,

In $q_{ce} = 4.218$, hence, $q_{ce} = e^{(4.218)}$

$q_{ce} = 67.90$ ppm

The result above shows a pseudo-first order rate constant $K_1 = 0.036$ ppm/min; while the calculated equilibrium adsorption, $q_{ce} = 67.90$ ppm and correlation coefficient value $R^2 = 0.770$

3.5.2 Pseudo-second-order kinetics of PNP-CHAC system

The linearized form of pseudo-second-order kinetics equation is also reported in chapter 2. From that equation, the plot of t/q_t against t should give a linear relationship. The q_{ce} and k_2 can be determined from the slope and intercept of the plot The Pseudo-second-order kinetics results of PNP-CHAC system are given in table 13

Table 13 pseudo second order kinetics of PNP-CHAC system

q_e = 64.65 constant for all the data: the amount of PNP adsorbed at equilibrium

t(mins)	Adsorption capacity of PNP in time t, q_t, ppm	q_e-q_t	ln (q_e-q_t)	t/ q_t
20	44.950	19.70	2.980	0.444
40	48.112	16.54	2.805	0.831
60	50.080	14.45	2.671	1.198
80	58.200	6.45	1.864	1.375
100	63.160	0.81	-0.210	1.583

The graphical representation of the above table is shown in fig. 11. A plot of t/qt against t mins gave a linear relationship whose slope and intercept are used to calculate q_{ce} and k_2 respectively.

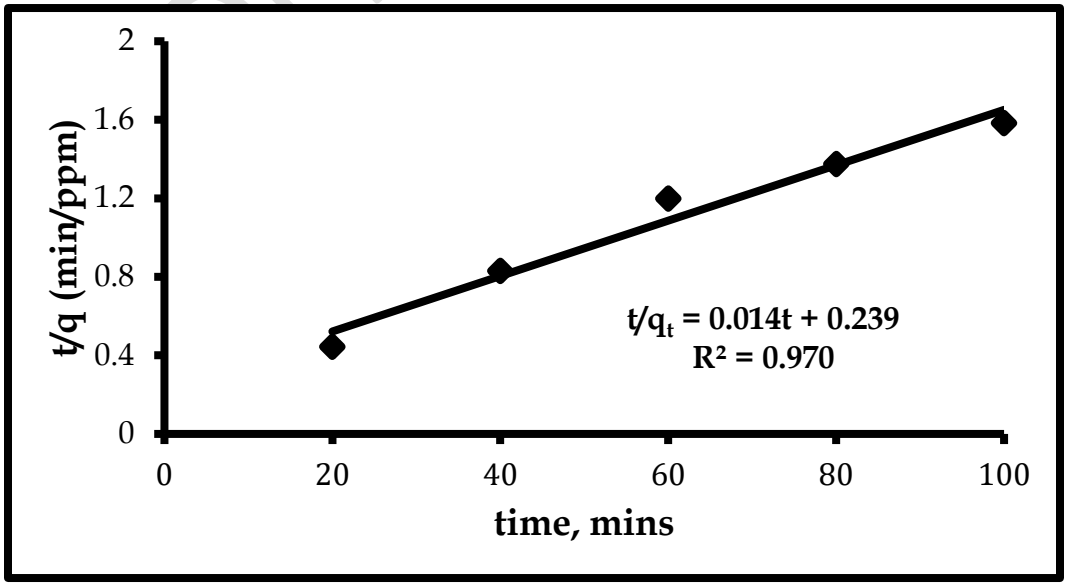

Fig 11 Pseudo-second order kinetics of PNP on CHAC

From the plot above,

$\frac{t}{q_t} = \frac{1}{k_2\ q_{ce}^2} + \frac{1}{q_{ce}}t$

$t/\ q_t = 0.014t + 0.239$

Comparing the above equations,

$1/q_{ce} = 0.014$, hence,

$q_{ce} = 71.42$ ppm

$1/\ (k_2\ q_{ce}^2) = 0.239 \qquad k_2 = 1/\ (q_{ce}^2 \text{ x } 0.239)$

$k_2 = 0.00082 = 8.2 \text{ X } 10^{-4}$ ppm/min

From result of the above graph, it was observed that the experimental second order rate constant is $K_2 = 8.2 \text{ X } 10^{-4}$ ppm/min, R^2 is 0.970 and calculated equilibrium adsorption amount, $q_{ce,}$ is 71.42 ppm. The adsorption process of 4-Nitrophenol on CHAC favors a second order mechanism as to first order, in respect to the above kinetic parameters.

3.5.3 Pseudo first order kinetics of PCP on CHAC

The linearized form of pseudo-first-order kinetics equation is reported in 2.4 From that equation it is clear that, a plot of ln (q_e - q_t) against t (mins) should give a linear relationship with the slop k_1 and intercept of $\ln q_{ce}$. The q_e value for PNP was taken as 67.31 ppm, the amount of PCP adsorbed at equilibrium as previously reported in table 7. The results of Pseudo-first-order kinetics of PCP-CHAC system is given below (Table 14)

Table 14 pseudo first order kinetics of PCP onto CHAC

q_e = 67.31 constant for all the data: the amount of PCP adsorbed at equilibrium.

Time, mins	**q_t, ppm**	**q_e-q_t**	**ln (q_e-q_t)**
20	47.65	19.66	2.979
40	51.33	15.98	2.771

60	54.74	12.57	2.531
80	59.42	7.89	2.066
100	66.15	1.16	0.148

The graphical illustration of the table above is presented in fig. .12 below. The plot of ln (q_e-q_t) on the vertical axis against time (mins) on the horizontal axis gives a linear relationship. The linear equation can be compared to that of the linearized pseudo-first order kinetics equation. The pseudo first order constant and the amount of adsorbate adsorbed at equilibrium can be calculated from the slope and intercept respectively.

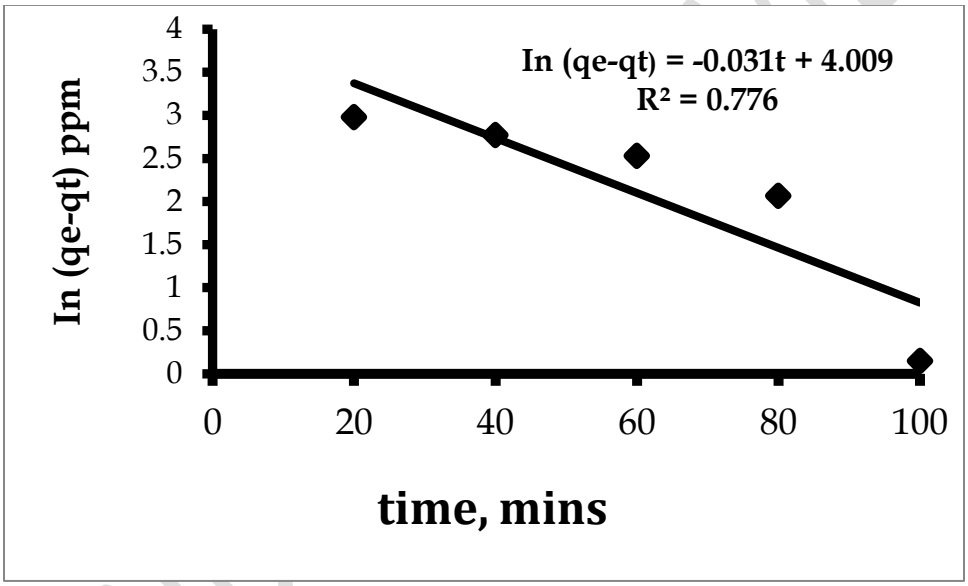

Fig .12 Pseudo- first order kinetics of PCP on CHAC

In (q_e-q_t) = Inq_{ce}-k_1t

In (q_e-q_t) = -0.031t + 4.009

Comparing both equations

In q_{ce} = 4.009 q_{ce} = e $^{(4.009)}$

q_{ce} = 55.09 ppm

Also,

$-K_1 = -0.031$,

$k_1 = 0.031$ ppm/min

The result from the graph above shows first order rate constant K_1 =0.031, the experimental first order calculated equilibrium concentration, q_{ce} = 55.09 ppm and correlation coefficient R^2 = 0.776.

3.5.4 Pseudo-second-order kinetics of PCP-CHAC system

The linearized form of pseudo-second-order kinetics equation is reported in 2.4 From the equation, the plot of t/q against t should give a linear relationship. The q_e and k_2 can be determined from the slope and intercept of the plot The Pseudo-second-order kinetics of PCP-CHAC system is given in table 15

Table 15 pseudo-second order kinetics data of PCP onto CHAC

q_e = 67.31 constant for all the data: the amount of PCP adsorbed at equilibrium.

Time, mins	q_t, ppm	q_e-q_t	ln (q_e-q_t)	t/q_t
20	47.65	19.66	2.979	0.419
40	51.33	15.98	2.771	0.779
60	54.74	12.57	2.531	1.096

80	59.42	7.89	2.066	1.346
100	66.15	1.16	0.148	1.512

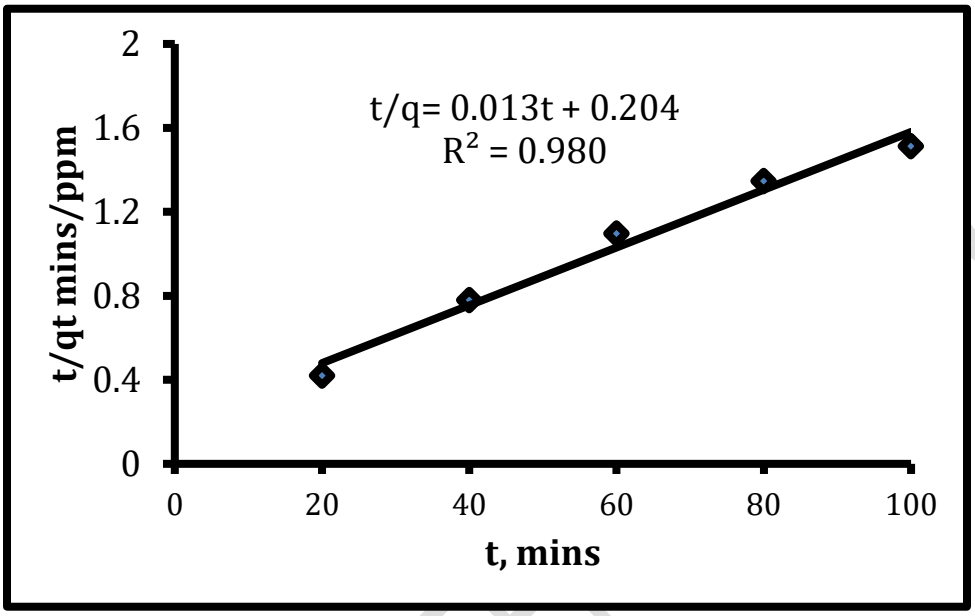

Fig .13 Pseudo-Second order kinetics of PCP on CHAC

From the above graph, the linear relationship can be compared to the linearized form of pseudo-second order kinetics equation

$\frac{t}{q_t} = \frac{1}{k_2\ q_{ce}^2} + \frac{1}{q_{ce}}t$ = t/qt = 0.013t + 0.204

Comparing the above equations,

$1/q_{ce} = 0.013$, hence,

$q_{ce} = 76.92$ ppm

$1/ (k_2\ q_e^2) = 0.204$ $k_2 = 1/ (q_{ce}^2 \text{ x } 0.204)$

$k_2 = 0.0008285$ ppm/min $= 8.285 \text{ X } 10^{-4}$ ppm/min

The result from the graph above shows pseudo-second order rate constant K_2 =8.285x10^{-4} ppm/min, the experimental second order calculated equilibrium concentration, q_{ce} = 76.92 ppm and correlation coefficient R^2 = 0980.

The summary of the kinetic studies for PCP and PNP on CHAC is shown in table 16.

R^2_2 = correlation coefficient for pseudo second order kinetics

R^2_1 = correlation coefficient for pseudo first order kinetics

Table 16 Summary of kinetic studies of phenolic derivatives on CHAC

	q_e, ppm	**q_{ce1} ppm**	**q_{ce2}, ppm**	**k_1 (ppm/min)**	**k_2 ppm/min**	**R^2_1**	**R^2_2**
PCP-CHAC system	67.31	55.09	76.92	0.031	8.285 X 10^{-4}	0.776	0.980
PNP-CHAC system	64.65	67.90	71.42	0.036	8.20 X 10^{-4}	0.770	0.970

From the results of kinetic studies shown in table 16, PCP fitted slightly better than PNP in the pseudo first order and second order kinetics plot. Also PCP has a higher second order rate constant than PNP, the experimental and calculated equilibrium concentrations for second order for PCP were also higher than that of PNP and this could be attributed to the lower molecular weight of PCP with respect to PNP.

Conclusions

The kinetics and equilibrium studies of detoxifying aqueous solutions of p-nitrophenol and p-chlorophenol on activated carbon from coconut husk have been investigated. In each case, the adsorbate adsorbed increased with the adsorbent dose. However, adsorption was optimal at an adsorbent dose of 0.2 g in each case. The adsorption capacity of the adsorbent decreased with

increased temperature in each case. This suggests that the adsorption is exothermic. Results of equilibrium analysis show that PNP has a higher maximum adsorption capacity, qo = 125 ppm, compared to PCP, which has a maximum adsorption capacity of qo = 71.43 ppm. Langmuir constant of adsorption was k_l = 9.44x10-3 ppm-1 for PNP and kl = 0.013 ppm-1 for PCP. The results above suggest that the adsorption process is consistent with the Langmuir isotherm model, which indicates monolayer adsorption of each of the adsorbates on the adsorbent. Kinetics studies show R^2 = 0.980 for the pseudo-second-order PCP-CHAC system and R^2 = 0.970 for the second-order PNP-CHAC system, indicating a good fit kinetic model for pseudo-second-order compared to the pseudo-first-order kinetic model in which R^2 = 0.776 and R^2 = 0.770 for PCP and PNP respectively. The pseudo-second-order suitably describes the kinetic system of the adsorbates on the adsorbent. The rate constants k_2 = 8.285 X 10^{-4} ppm/min for the PCP-CHAC system and k_2 = 8.20 X 10^{-4} ppm/min for the PNP-CHAC system show that adsorption of PCP onto CHAC is faster than PNP onto CHAC and this could be attributed to the lower molecular weight of PCP.

DISCLAIMER (ARTIFICIAL INTELLIGENCE)

Author(s) hereby declare that NO generative AI technologies such as Large Language Models (ChatGPT, COPILOT, etc) and text-to-image generators have been used during writing or editing of manuscripts.

CONSENT

As per international standards or university standard, patient(s) written consent has been collected and preserved by the author(s).

ETHICAL APPROVAL

As per international standards or university standard written ethical approval has been collected and preserved by the author(s).

References:

Adeniji, A. E., Osundiran, F. J., Ayoola, O. G., Adeogun, A. I., & Idowu, M. A. (2021). KINETIC AND THERMODYNAMIC STUDIES OF REMOVAL OF 2-NITROPHENOL FROM AQUEOUS

SOLUTION USING COWPEA HUSK POWDER TETHERED ON IRON OXIDE.*Journal of Chemical Society of Nigeria*, *46*(6).

Adeola, A. O. (2018). Fate and toxicity of chlorinated phenols of environmental implications: a review. *Medicinal and analytical chemistry international journal*, *2*(4), 000126.

Adetunji, C. O., Olaniyan, O. T., Igere, B. E., Ekundayo, T. C., Anani, O. A., Bodunrinde, R. E., ... & Inamuddin. (2021). Microbial Degradation of Chlorophenolic Compounds. *Recent Advances in Microbial Degradation*, 313-349.

Al-Ahmadi, M. S. (2022). Effects of 2-chlorophenol and 2, 4-dichlorophenol on mitotic chromosomes and nucleic acid content using Allium cepa and Vicia faba assays.

Anjum, N., Ridwan, Q., Rashid, S., Akhter, F., & Hanief, M. (2022). Microbial degradation of organophosphorus pesticides. In *Bioremediation and Phytoremediation Technologies in Sustainable Soil Management* (pp. 159-185). Apple Academic Press.

Anwar, S., & Li, X. (2024). A review of high-quality epoxy resins for corrosion-resistant applications. *Journal of Coatings Technology and Research*, *21*(2), 461–480.

Azari, A., Nabizadeh, R., Mahvi, A. H., & Nasseri, S. (2022). Integrated Fuzzy AHP-TOPSIS for selecting the best color removal process using carbon-based adsorbent materials: multi-criteria decision making vs. systematic review approaches and modeling of textile wastewater treatment in real conditions. *International Journal of Environmental Analytical Chemistry*, *102*(18), 7329-7344.

Brillas, E. (2020). A review on the photoelectro-Fenton process as efficient electrochemical advanced oxidation for wastewater remediation. Treatment with UV light and sunlight and coupling with conventional and other photo-assisted advanced technologies. *Chemosphere*, *p. 250*, 126198.

Ekpete O. A., Horsfall Jnr M. and Tarawou T. (2011). Sorption kinetic study on the removal of phenol using fluted pumpkin and commercial activated carbon, Int. J. Biol. Chem. Sci. 5(3): 1143-1152.

Fernández, S. F., Pardo, O., Adam-Cervera, I., Montesinos, L., Corpas-Burgos, F., Roca, M., ... & Yusà, V. (2020). Biomonitoring of non-persistent pesticides in urine from lactating mothers: Exposure and risk assessment. *Science of the Total Environment*, *699*, 134385.

Garba, Z. N., Zhou, W., Lawan, I., Xiao, W., Zhang, M., Wang, L., ... & Yuan, Z. (2019). An overview of chlorophenols as contaminants and their removal from wastewater by adsorption: A review. *Journal of environmental management*, *241*, 59-75.

Ghatbandhe A.S., Yenkie M.K.N., Jahagirdar H.G. and Deosarkar S.D. (2009). Sorption Equilibrium and Kinetic Studies of P-Chlorophenol from Aqueous Solution Using Granular Activated Carbon and Studies on Effect of Temperature on Adsorption, American-Eurasian Journal of Scientific Research 4 (3): 159-164

Gijjapu, D. R., & Nazal, M. K. (2023). Ionic liquids for phenolic compounds removal and extraction. In *Green Sustainable Process for Chemical and Environmental Engineering and Science* (pp. 217-238). Elsevier.

Husieva, A. V. (2021). *Photocatalytic treatment of wastewater contaminated with aromatic compounds* (Doctoral dissertation, National Aviation University).

Irshad, M. A., Sattar, S., Nawaz, R., Al-Hussain, S. A., Rizwan, M., Bukhari, A., ... & Zaki, M. E. (2023). Enhancing chromium removal and recovery from industrial wastewater using sustainable and efficient nanomaterial: a review. *Ecotoxicol Environ Saf*, *263*(115231), 10-1016.

Joseph, J. K., Naiker, V., Sreeram, P., Mampulliyalil, F., Varghese, P. G., Dhawale, P. V., ... & Raghavan, P. (2024). Phenolic resin: Preparation, structure, properties, and applications. In *Handbook of Thermosetting Foams, Aerogels, and Hydrogels* (pp. 383–420). Elsevier.

Lojo-López, M., Andrades, J. A., Egea-Corbacho, A., Coello, M. D., & Quiroga, J. M. (2021). Degradation of simazine by photolysis of hydrogen peroxide Fenton and photo-Fenton under darkness, sunlight, and UV light. *Journal of Water Process Engineering*, *42*, 102115.

Marussi, G., & Vione, D. (2021). Secondary formation of aromatic nitro derivatives of environmental concern: photonitration processes triggered by the photolysis of nitrate and nitrite ions in aqueous solution. *Molecules*, *26*(9), 2550.

Mir, I. A., Ain, Q. U., Qadir, T., Malik, A. Q., Jan, S., Shahverdi, S., & Nabi, S. A. (2023). A review of semicarbazone-derived metal complexes for application in biomedicine and related fields. *Journal of Molecular Structure*, 136216.

Moreno Gracia B, Laya Reig D, Rubio-Cabetas MJ, Sanz García MÁ. Study of Phenolic Compounds and Antioxidant Capacity of Spanish Almonds. Foods. 2021 Sep 30;10(10):2334. doi: 10.3390/foods10102334.

Msagati, T. A. (2017). *Food Forensics and Toxicology*. John Wiley & Sons.

Panigrahy, N., Priyadarshini, A., Sahoo, M. M., Verma, A. K., Daverey, A., & Sahoo, N. K. (2022). A comprehensive review on eco-toxicity and biodegradation of phenolics: Recent progress and future outlook. *Environmental Technology & Innovation*, *p. 27*, 102423.

Patrick, A. O., Ozioma, O. E., Shine, G. K., Michael, A. T., Nwosu, S. N., Bassey, E. B., ... & Tochi, N. S. (2024). Proximate Analysis, Extraction, and Characterization of Oil from Terminalia catappa Fruit in Anambra State, Nigeria. *Asian Journal of Research in Biochemistry*, *14*(4), 126-137. DOI: https://doi.org/10.9734/ajrb/2024/v14i4301

Pizzi, A., & Ibeh, C. C. (2022). Phenol-formaldehyde resins. In *Handbook of Thermoset Plastics* (pp. 13-40). William Andrew Publishing.

Ramos, R. L., Moreira, V. R., Lebron, Y. A., Santos, A. V., Santos, L. V., & Amaral, M. C. (2021). Phenolic compounds seasonal occurrence and risk assessment in surface and treated waters in Minas Gerais—Brazil. *Environmental Pollution*, *268*, 115782.

Sivaraman, C., Vijayalakshmi, S., Leonard, E., Sagadevan, S., & Jambulingam, R. (2022). Current developments in the effective removal of environmental pollutants through photocatalytic degradation using nanomaterials. *Catalysts*, *12*(5), 544.

Skowroń, J. (2020). Carcinogenic and Mutagenic Substances. In *Emerging Chemical Risks in the Work Environment* (pp. 127-166). CRC Press.

Sujiono, E. H., Zabrian, D., Zharvan, V., & Humairah, N. A. (2022). Fabrication and characterization of coconut shell activated carbon using variation chemical activation for wastewater treatment application. *Results in Chemistry*, *4*, 100291.

Szafran, B., Klein, R., Buser, M., Balachandran, R., Haire, K., Derrick, H., ... & Citra, M. (2023). Toxicological profile for nitrophenols.

Trisunaryanti, W., Wijaya, K., Triyono, T., Wahyuningtyas, N., Utami, S. P., & Larasati, S. (2022). Characteristics of coconut shell-based activated carbon as Ni and Pt catalyst supports for hydrotreating Calophyllum inophyllum oil into hydrocarbon-based biofuel. *Journal of Environmental Chemical Engineering*, *10*(5), 108209.

Underwood, L. A. (2018). Properties, functionality and potential applications of novel modified iron nanoparticles for the treatment of 2, 4, 6-Trichlorophenol.

Vallant, D. (2016). Degradation of model reactants as a chemical probe for cavitation-induced hot spots in water treatment devices.

Yadav, S., & Maurya, P. K. (2022). Recent advances in the protective role of metallic nanoparticles in red blood cells. *3 Biotech*, *12*(1), 28.

Zaki, M. S., Hammam, A. M., Yousef, R. A., Fawzi, O., & Shalaby, S. S. (2015). Phenols and phenolic compounds: sources, routes of exposure and mode of action. *Advances in Environmental Biology*, *9*(8), 49-58.

Zhu, B., Jiang, X., Li, S., & Zhu, M. (2024). An Overview of Recycling Phenolic Resin. *Polymers*, *16*(9), 1255.